PEGylation Does Not Significantly Change the Initial Intravenous or Subcutaneous Pharmacokinetics or Lymphatic Exposure of Trastuzumab in Rats but Increases Plasma Clearance after Subcutaneous Administration

Linda J. Chan,[†] Jürgen B. Bulitta,[†] David B. Ascher,[‡] John M. Haynes,[§] Victoria M. McLeod,[†] Christopher J. H. Porter,[†] Charlotte C. Williams,[||] and Lisa M. Kaminskas*,[†]

[†]Drug Delivery, Disposition and Dynamics, Monash Institute of Pharmaceutical Sciences, Monash University, 381 Royal Parade, Parkville, Victoria 3052, Australia

[‡]Department of Biochemistry, University of Cambridge, Sanger Building, Downing Site, Cambridge, CB2 1GA, U.K.

[§]Drug Discovery Biology, Monash Institute of Pharmaceutical Sciences, Monash University, 381 Royal Parade, Parkville, Victoria 3052, Australia

[||]CSIRO Materials Science and Engineering, 343 Royal Parade, Parkville, Victoria 3052, Australia

Ⓢ *Supporting Information*

ABSTRACT: The lymphatic system plays a major role in the metastatic dissemination of cancer and has an integral role in immunity. PEGylation enhances drainage and lymphatic uptake following subcutaneous (sc) administration of proteins and protein-like polymers, but the impact of PEGylation of very large proteins (such as antibodies) on subcutaneous and lymphatic pharmacokinetics is unknown. This study therefore aimed to evaluate the impact of PEGylation on the sc absorption and lymphatic disposition of the anti-HER2 antibody trastuzumab in rats. PEG–trastuzumab was generated via the conjugation of a single 40 kDa PEG-NHS ester to trastuzumab. PEG–trastuzumab showed a 5-fold reduction in HER2 binding affinity, however the *in vitro* growth inhibitory effects were preserved as a result of changes in cellular trafficking when compared to native trastuzumab.

Lymphatic disposition of PEG-trastuzumab post SC dosing

The lymphatic pharmacokinetics of PEG–trastuzumab was evaluated in thoracic lymph duct cannulated rats after iv and sc administration and compared to the pharmacokinetics of native trastuzumab. The iv pharmacokinetics and lymphatic exposure of PEG–trastuzumab was similar when compared to trastuzumab. After sc administration, initial plasma pharmacokinetics and lymphatic exposure were also similar between PEG–trastuzumab and trastuzumab, but the absolute bioavailability of PEG–trastuzumab was 100% when compared to 86.1% bioavailability for trastuzumab. In contrast to trastuzumab, PEG–trastuzumab showed accelerated plasma clearance beginning approximately 7 days after sc, but not iv, administration, presumably as a result of the generation of anti-PEG IgM. This work suggests that PEGylation does not significantly alter the lymphatic disposition of very large proteins, and further suggests that it is unlikely to benefit therapy with monoclonal antibodies.

KEYWORDS: *PEGylation, trastuzumab, lymphatic, pharmacokinetics, monoclonal antibody, HER2, population modeling, S-ADAPT*
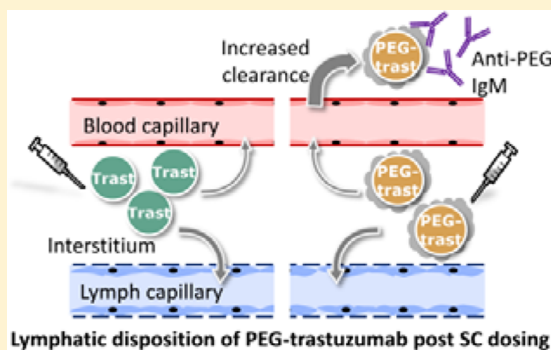
■ INTRODUCTION

Monoclonal antibodies (mAbs) are becoming increasingly important therapeutics in the treatment of cancer, heart disease, and inflammation, with annual profits amounting to billions of dollars.[1,2] Breast cancer is the most common form of cancer affecting women worldwide, and human epidermal growth factor receptor 2 (HER2) overexpressing breast cancers in particular are associated with an increased risk of metastasis and poor clinical prognosis for the patient.[3] Trastuzumab is a 150 kDa mAb currently in use for the treatment of early and metastatic HER2-positive breast cancers.[4,5] It contains two antigen-specific sites that bind to the HER2 extracellular

domain and inhibits the proliferation of tumor cells that overexpress HER2.

The lymphatic system is a major conduit by which breast cancers metastasize, and lymphadenectomy is commonly performed as a preventative measure to limit the metastatic spread of HER2 positive cancers.[6] This procedure is associated with significant morbidity, however, and there is evidence to suggest that this intervention has a poor success rate in

A

preventing the metastatic spread of the disease.[6,7] Lymphadenectomy is also performed, however, to inform the stage of tumor progression (stage 1 through 4), thus the removal of lymph nodes for staging purposes cannot be entirely avoided.[8] Intravenous (iv) chemotherapy alone, however, would provide insufficient drug access to the lymph, which may limit the successful treatment of cancers where lymphatic metastasis is a significant contributor to disease progression (such as for breast cancer).[9] Therefore, there is significant interest in identifying approaches that can improve the lymphatic disposition of small molecule and protein-based drugs which also retains intrinsic biological activity.

The current standard dosing route for trastuzumab is iv, which requires administration by trained medical personnel. We recently showed that trastuzumab efficiently targets the lymph of rats after iv dosing, but also demonstrated that subcutaneous (sc) administration can significantly improve the exposure of the antibody to lymphatic vessels and nodes downstream from the injection site when compared to iv administration,[10] despite incomplete sc absorption. This has similarly been shown for other proteins and drug delivery systems.[11−13] The sc administration of trastuzumab and other protein-based therapeutics used in the treatment of cancer (such as immunomodulators) near the site of a primary tumor may therefore provide a useful means of improving the treatment of lymph metastatic cancers and avoid the need for the prophylactic removal of sentinel lymph nodes. Furthermore, in 2013, a sc formulation containing trastuzumab and recombinant human hyaluronidase was approved for clinical use in Europe, and it is expected to extend absorption time, allowing for less frequent and more convenient dosing.[14,15]

While the sc administration of trastruzumab and other mAbs with indications against various cancers may provide a means of efficiently targeting lymph-resident cancers and metastases, the bioavailability of proteins after sc administration is typically variable, and the determinants that contribute to such variability are still largely undefined.[16,17] Several factors can affect the absorption and bioavailability of proteins after sc administration, including molecular weight,[18] the presence of formulation excipients,[11] and convection away from,[19,20] and interstitial pressure at, the injection site.[21,22] At present, the molecular weight or size of a protein is thought to be a primary determinant of the route of absorption into either the blood or the lymph.[11] Proteins larger than 16−20 kDa are preferentially absorbed via the lymphatic system, while smaller proteins are absorbed via the vascular capillaries.[18] As molecular weight increases, so too does the fraction of an sc dose that is taken up into the peripheral lymphatics.[23−26] For mAbs, interactions between the antibody and FcRn receptors can also have an impact on absorption and in vivo stability, since the intracellular binding of antibodies with FcRn receptors protects the antibody from cellular proteases while transcytosing through cells.[27]

Recent studies have suggested that the conjugation of polyethylene glycol (PEG) can also improve convection of macromolecules from sc injection sites and improve bioavailability and uptake via the lymphatics.[12,13] This is believed to be due to increases in molecular hydrophilicity promoting better drainage from the injection site via aqueous channels in the extracellular matrix, and possibly enhancing the rate of paracellular transport through vascular and lymphatic endothelia. PEGylation can also prolong the circulation half-life of proteins by increasing the effective size of the protein (thereby restricting extravasation) and reducing proteolytic degradation.[28] These potential benefits have been exploited for a number of bioactive enzymes and proteins and have led to the development of several PEGylated macromolecular drug conjugates that are either on the market or in clinical development.[29] Furthermore, the PEGylation of antibodies has been shown in mouse tumor xenograft models to have the potential to increase disposition toward solid primary tumors and therefore improve chemotherapeutic activity.[30,31] This has been suggested to be via increases in molecular weight leading to more prolonged plasma exposure after iv administration and enhanced tumor uptake via the enhanced permeation and retention effect.[30,31] PEGylation therefore has the potential to improve the sc pharmacokinetic behavior of trastuzumab and increase lymphatic and solid tumor disposition. To this point, however, the impact of PEGylation on the sc pharmacokinetics and lymphatic disposition of very large proteins, such as antibodies, has not been explored. Further work is also required to understand how PEGylation alters receptor binding kinetics and biological activity of antibodies.

The first objective of the current study was therefore to prepare mono-PEGylated trastuzumab with minimal PEG loading of approximately 20% w/w and compare its receptor binding affinity, cellular trafficking, and in vitro growth inhibitory effects to those of native trastuzumab. To achieve this, we chose to conjugate a single linear 40 kDa methoxy-PEG to trastuzumab, rather than conjugate many smaller (e.g., 5 kDa) PEGs, since (1) the conjugation of multiple smaller PEGs may inhibit receptor recognition to a greater degree than the conjugation of a single larger PEG, (2) the conjugation of single PEGylated species is a common approach employed to prepare PEGylated protein-based therapeutics, and (3) this approach was expected to have a greater synthetic yield of a single product when compared to the conjugation of multiple smaller PEGs.[32,33] Second, the sc absorption, bioavailability, and lymphatic disposition of PEG−trastuzumab were investigated in thoracic lymph duct cannulated rats. This is important to evaluate whether there is likely any therapeutic benefit to PEGylating trastuzumab in the context of changes in sc or lymphatic pharmacokinetics. The disposition of PEG−trastuzumab and trastuzumab in plasma and lymph was subsequently compared using population pharmacokinetic modeling and simulation. It was anticipated that increasing the molecular size and hydrophilicity of trastuzumab via PEGylation would favor selective delivery to the peripheral lymphatics after sc administration and improve bioavailability. This has the potential to target anticancer efficacy against cells that proliferate within the lymph and thus improve therapy for HER2-positive breast cancers.

■ EXPERIMENTAL SECTION

Reagents and Supplies. Trastuzumab (Trastuzumab) was purchased from Roche Pty Ltd. (Dee Why, NSW, Australia) as a lyophilized product, and linear methoxy PEG succinimidyl carboxymethyl ester (NHS-PEG, with an average molecular weight of 40 kDa) was from JenKem Technology (Plano, TX, USA). BT474 and T47D cells were kindly provided by Dr. Mark Waltham at St Vincent's Institute of Medical Research (VIC, Australia). Human umbilical vein endothelial cells (HUVECs) and sterile EGM-2 media kit were purchased from Lonza (Mt Waverley, VIC, Australia). Human IgG ELISA kits were obtained from Mabtech (Thomastown, VIC, Australia). DMSO, thiazolyl blue tetrazolium bromide, and p-

nitrophenyl phosphate tablets were from Sigma-Aldrich (Castle Hill, NSW, Australia). Polyacrylamide gels (4−12% Bis-Tris) and molecular weight markers were from Life Technologies (Mulgrave, VIC, Australia). Cell culture reagents were purchased from Gibco Life Technologies. Polyvinyl, polyethylene, and silastic medical grade tubing (internal diameter 0.58 mm, external diameter 0.96 mm) were obtained from Microtube Extrusions Pty Ltd. (NSW, Australia). All other buffer reagents were purchased from Ajax Finechem Pty Ltd. (NSW, Australia) and were analytical grade.

Animals. Male Sprague−Dawley rats (250−320 g) were obtained from Monash Animal Services (Clayton, VIC, Australia) and maintained in a controlled environment with a 12 h light/dark cycle. Water was provided *ad libitum*. Food was withheld post surgical cannulation and for 8 h after dosing, but was provided freely at all other times. All animal experimental procedures were approved by the Monash Institute of Pharmaceutical Sciences Animal Ethics Committee.

Preparation of Mono-PEGylated Trastuzumab. Trastuzumab (150 mg) was reconstituted in 7.2 mL of sterile water to obtain a final concentration of 21 mg/mL. The reconstituted trastuzumab was buffer exchanged into the PEGylation reaction buffer (sterile phosphate buffered saline (PBS) containing 0.5 mM EDTA, pH 7.2) to remove all excipients. The 40 kDa PEG-NHS was dissolved in sterile water at 10 mg/mL. The PEGylation reaction was carried out at 1:5 molar equiv of trastuzumab:PEG in an endotoxin-free eppendorf tube and incubated overnight at 4 °C without shaking. This reaction gives a PEGylated product that is stably conjugated to the protein. PEG−trastuzumab was then purified under "endotoxin-in-minimizing conditions" using size exclusion chromatography on a Superdex 200 HR 10/30 column at a flow rate of 0.5 mL/min with PBS containing 0.5 mM EDTA as the mobile phase over 60 min. Contamination of the final product by bacterial lipopolysaccharides was minimized by sterile filtering and autoclaving the mobile phase and washing columns prior to use with 2 M NaCl/1 M NaOH for an hour, which removes endotoxin contamination. In addition, where possible, sterile and endotoxin free consumables were used following purification of the PEGylated product. The level of endotoxin contamination in the final PEG−trastuzumab product was quantified using a Pierce Limulus Amebocyte Lysate (LAL) assay kit (Thermo Scientific, Scoresby, VIC, Australia), which was used according to the manufacturer's instructions. Endotoxin levels in the final product were determined to be below 1 EU/mg protein. The identity of the purified mono-PEG−trastuzumab was confirmed by reducing and non-reducing SDS−PAGE (Figure S1, Supporting Information) and mass spectrometry on an Agilent Q-TOF LC/MS with a C8 column and a gradient of 5−75% acetonitrile in 0.1% formic acid. Mass spectrometry data was deconvoluted using Mass-Hunter qualitative analysis software (Agilent).

Size Exclusion Chromatography Multiangle Light Scattering (SEC-MALS). SEC-MALS analysis was performed to determine the experimental molecular weight of the soluble PEGylated species. PEG−trastuzumab (0.15 μg in 50 μL) was run on a Tosoh TSKgel SuperSW2000 4.6*300 mm column equilibrated in PBS at a flow rate of 0.35 mL/min using a Shimadzu LC-20AD isocratic HPLC coupled to a Dawn Heleos MALS detector and an Optilab T-rEX refractive index detector (Wyatt Technology). The molecular weight and degree of PEGylation were determined according to the three-detector method[34] using the ASTRA 5 software (Wyatt Technologies).

Microscale Thermophoresis (MST). Solution MST binding studies were performed to measure the effect of PEGylation on the binding affinity of trastuzumab for HER2 using standard protocols on a Monolith NT.115 (Nanotemper Technologies).[35] The HER2 was labeled using a RED-NHS (Amine Reactive) Protein Labeling Kit (Nanotemper Technologies) which contains an NT-647 dye. Labeled HER2 was mixed with either trastuzumab or PEGylated trastuzumab in PBS with 0.05% Tween-20. Each replicate contained a 16 step 2-fold serial dilution series. The HER2 protein concentration (1 nM) was chosen such that the observed fluorescence was approximately 400 units at 70% LED power. The samples were loaded into standard capillaries and heated at 40% laser power for 30 s, followed by 5 s cooling. The data were normalized against the baseline obtained in the absence of any trastuzumab, and the maximal response obtained at the highest concentration of inhibitor. The dissociation constant K_D was obtained by plotting the normalized fluorescence F_{norm} against the logarithm of the concentrations of the dilution series resulting in a sigmoidal binding curve that could be directly fitted with a nonlinear solution of the law of mass action. All experiments were performed with a minimum of 3 replicates, and the normalized fluorescence thermophoresis curves were analyzed using GraphPad Prism (Version 6, GraphPad, San Diego, CA, USA). K_D values were compared to the non PEGylated trastuzumab by t test, with $p < 0.05$ considered to be statistically significant.

***In Vitro* Growth Inhibitory Effects of PEG−Trastuzumab and Trastuzumab.** The ability of PEG−trastuzumab and native trastuzumab to inhibit the growth of HER2 positive (BT474) and HER2 negative (T47D) human breast cancer cells was compared *in vitro*. BT474 and T47D cells were maintained in RPMI medium supplemented with 10% fetal bovine serum, 10,000 U/mL penicillin, 10,000 mg/L streptomycin, and GlutaMAX (Gibco). Cells were washed with sterile Dulbecco's phosphate-buffered saline (DPBS) prior to trypsinization with 0.25% trypsin−EDTA. Cells (5,000 per well) were seeded in 96-well plates and treated the following day with 0 to 100 μg/mL of PEG−trastuzumab or trastuzumab. After 3 days, cell viability was assessed via the addition of 10 μL of thiazolyl blue tetrazolium bromide (MTT) (5 mg/mL) per well for 2 h at 37 °C. The absorbance of each well was measured using an EnSpire plate reader (PerkinElmer) at 590 nm. Cell viability was expressed relative to the untreated control at t_0 as previously described.[36] Cell viability curves were best fitted using a sigmoidal dose−response (inhibition) curve on GraphPad Prism.

Cellular Trafficking of PEG−Trastuzumab in BT474 Cells. Cell binding and endocytosis of fluorescent-labeled trastuzumab and PEG−trastuzumab in BT474 cells was assessed via confocal microscopy (Nikon A1R confocal microscope) in the presence of intracellular markers, including the early endosome marker Early Endosome Antigen 1 (EEA1, Abcam, Waterloo, NSW, Australia). Trastuzumab and PEG−trastuzumab were fluorescently labeled using an Alexa Fluor 488 (Alexa488) Protein Labeling Kit (Life Technologies, Mulgrave, VIC, Australia) according to the manufacturer's instructions. Centrifugal filters with a 10 kDa molecular weight cutoff (Millipore, Darmstadt, Germany) were used to buffer exchange Alexa488−trastuzumab and PEG−trastuzumab into PBS containing 0.5 mM EDTA. The final Alexa-labeled products were confirmed by SDS−PAGE and were shown to

be similar in molecular weight to the unmodified antibodies (see Figure S1, Supporting Information).

For imaging studies, BT474 cells (2,500 cells) were seeded onto glass bottom culture dishes coated with rat tail collagen (type I) the day before incubation with the test compounds. Alexa488−trastuzumab or Alexa488−PEG−trastuzumab (1 μg/mL of protein, since conjugation of Alexa488 did not significantly alter molecular weight) was added and incubated for 48 h at 37 °C in a humidified environment at 5% CO_2. Cells were then fixed with 4% paraformaldehyde in PBS and left for 10 min at room temperature, after which cells were washed 3 times with PBS prior to the addition of the blocking/permeabilizing solution (10% donkey serum, 0.3% TritonX in PBS for 1 h). Primary anti-EEA1 antibody was added at 1 μg/mL and left overnight at 4 °C. Cells were again washed 3 times with PBS prior to the addition of donkey anti-mouse IgG H&L Alexa Fluor 647 conjugated secondary antibody (1:1,000 dilution). Cells were stored at 4 °C in the dark until imaged.

Lymphatic Pharmacokinetics of PEG−Trastuzumab after Iv and Sc Administration in Rats. The pharmacokinetics of PEG−trastuzumab were assessed in six groups of rats (n = 4−5) via a parallel design study. The groups comprised (1) iv-dosed long-term controls; (2) sc-dosed long-term controls; (3) iv-dosed short-term controls; (4) sc-dosed short-term controls; (5) iv-dosed thoracic lymph duct cannulated rats; and (6) sc-dosed thoracic lymph duct cannulated rats. Long-term control rats (groups 1 and 2) were not cannulated, and were housed in groups in microisolator cages for the duration of the study. Blood samples (150 μL) were collected via a lateral tail vein under isoflurane anesthesia on days 1, 3, and 7 and weekly from day 7 onward until day 49. Long-term control groups enabled assessment of the elimination half-life of PEG−trastuzumab after iv and sc dosing. Short-term control rats (groups 3 and 4) were cannulated via the right carotid artery to enable more frequent blood sampling over 7 days and were individually housed in metabolism cages. Iv-dosed short-term control rats (group 3) were also cannulated via the jugular vein to enable iv dosing. Thoracic lymph cannulated rats (groups 5 and 6) were cannulated via the right carotid artery (to enable blood sampling), the right jugular vein (to enable iv dosing and the replacement of fluid lost from the thoracic duct cannula via the constant infusion of 1.5 mL/h sterile saline), and the thoracic lymph duct approximately 1 cm below the diaphragm (to enable the continuous collection of lymph fluid entering the duct posterior to the cannula for 30 h after dosing) as described previously.[12,37] It is not feasible to continuously collect lymph for longer than approximately 48 h since the prolonged loss of plasma proteins via the lymph duct cannula may alter osmotic pressure of the vasculature and lead to edema (which would ultimately increase lymphatic fluid flow and potentially impact the pharmacokinetics of administered drugs and macromolecules).[38] Using the 30 h sampling protocol described here, however, we have previously achieved good mass balance recovery of small molecule drugs, proteins, and nanomaterials in lymph duct cannulated and noncannulated rats, suggesting that the 30 h sampling period gives reliable data.[10,12,13,39,40] All cannulae were then exteriorized to the back of the neck through a swivel-tether apparatus.

A blank blood sample (150 μL) was collected from all rats immediately prior to dosing into heparinized (10 IU) eppendorf tubes. Long-term control rats were dosed with 2 mg/kg PEG−trastuzumab as a bolus in sterile saline via a lateral

tail vein (500 μL volume) or sc into the inner left heel (in a volume of 0.5 mL/kg) under isoflurane anesthesia. Blood samples (150 μL) were then collected from a lateral tail vein (alternate vein to the one receiving the iv dose for iv dosed rats) 30 min, 1 d, 3 d, 7 d, 14 d, 21 d, 28 d, 35 d, 42 d, and 49 d later. Iv-dosed short-term control and thoracic lymph duct cannulated rats were administered PEG−trastuzumab at a dose of 2 mg/kg in 1 mL sterile saline via infusion over 2 min via the jugular vein. Sc-dosed short-term and thoracic lymph duct cannulated rats were administered PEG−trastuzumab as described above for sc dosed long-term rats. Blood samples were collected via the carotid artery cannula in short-term control rats immediately after dosing (t_0) and at 5 min, 30 min, 1 h, 2 h, 4 h, 8 h, 12 h, 24 h, 30 h, 2 d, 3 d, 4 d, 5 d, 6 d, and 7 d thereafter. Blood samples were collected from lymph duct cannulated rats at 5 min, 30 min, 1 h, 2 h, 3 h, 4 h, 6 h, 8 h, 12 h, 24 h, 27 h, and 30 h. Pooled thoracic duct lymph was collected over times 0−1 h, 1−2 h, 2−3 h, 3−4 h, 4−6 h, 6−8 h, 8−12 h, 12−24 h, 24−27 h, and 27−30 h as described previously.[10] All blood and lymph samples were kept on ice until further processed. Blood samples were centrifuged at 3500g for 5 min to obtain plasma. Plasma and lymph samples were stored at −20 °C prior to analysis.

Quantification of PEG−Trastuzumab in Plasma and Lymph. PEG−trastuzumab was quantified using a commercially available ELISA kit (Mabtech) for native human IgG. The ELISA was performed according to the manufacturer's instructions with minor modifications and was validated against both rat plasma and lymph. The validated concentration range was 0.5 to 300 ng/mL for both plasma and lymph. Briefly, microtiter plates (96-well, Costar, Corning) were coated with 100 μL of primary antibody (2 μg/mL) in phosphate buffered saline (PBS, 50 mM, pH 7.4) overnight at 4 °C. Wells were washed twice with PBS the following day and blocked with 200 μL of blocking buffer (PBS containing 0.05% Tween-20 and 0.1% bovine serum albumin (BSA)) for 1 h at room temperature. Wells were then washed five times with PBS containing 0.05% Tween-20 (PBS-Tween) prior to the addition of 100 μL PEG−trastuzumab standards and plasma and lymph samples. Standards and samples were prepared in blocking buffer, and standards were prepared containing a 1:100 dilution of either plasma or lymph. Plasma and lymph samples were prepared using appropriate dilutions (1:100 to 1:1,000). After a 2 h incubation at room temperature, wells were washed five times with PBS-Tween. Secondary antibody (100 μL, at 1:1,000 dilution) was added and incubated for 1 h at room temperature. After washing, 100 μL of p-nitrophenyl phosphate (pnPP) was added for 30 min. The absorbance for each well was quantified using an EnSpire plate reader at 405 nm.

Noncompartmental Pharmacokinetic Analysis. The noncompartmental pharmacokinetics of PEG−trastuzumab was determined using WinNonlin Pro (Version 5.3, Pharsight Corp., Mountain View, CA) as described previously.[10] Since the terminal elimination pharmacokinetics of PEG−trastuzumab could not be determined over 7 days in cannulated rats, the elimination rate constant (k) and half-life ($t_{1/2}$) in sc and iv dosed animals was determined in long-term rats. This enabled extrapolation of the area under the plasma concentration−time curve in short-term (7 day) sampled rats to infinity as described previously.[10]

Population Pharmacokinetic Modeling. To better understand and compare the absorption and disposition of PEG−trastuzumab and trastuzumab in plasma and lymph, a

population modeling approach was used. This enabled prediction of the concentration time profiles of each drug in plasma and lymph in non lymph cannulated (i.e., "control") rats (where lymph could not be sampled at later time points due to ethical and practical constraints). To obtain robust model parameter estimates, all plasma and lymph data for PEG–trastuzumab (this study) and trastuzumab (our previous study[10]) were simultaneously analyzed by population PK modeling. The plasma concentrations and fractions of dose collected in lymph during each dosing interval were modeled as described previously[10] using the S-ADAPT and SADAPT-TRAN software packages.[41−44]

Candidate model structures were based on our previous population PK models for lymph data.[10,40] Drug was absorbed from the sc injection site via first-order kinetics into the posterior peripheral lymph compartment and via first-order (for PEG–trastuzumab) or Michaelis–Menten kinetics (for trastuzumab) into the central compartment. Candidate models considered first-order and Michaelis–Menten elimination from the central compartment as well as, for PEG–trastuzumab, an immune response related clearance. The lymphatic exposure of PEG–trastuzumab in control and lymph cannulated rats after iv and sc dosing was predicted using the Berkeley Madonna software (version 8.3.18) to simulate the extensive distribution of drug transfer into lymph as described previously.[10]

Determination of Anti-PEG IgM Antibody Production after Iv and Sc Administration of PEG–Trastuzumab and Native Trastuzumab. The potential for PEG–trastuzumab to promote the generation of anti-PEG IgM antibodies after iv and sc administration to rats was examined via ELISA, and the results were compared to rats administered native trastuzumab.[45] Plasma samples from rats that provided data on the pharmacokinetics of native trastuzumab in the previous work were used here.[10] BSA (50 μL of 0.5 mg/mL) was added to each well of two 96-well microplates (Medisorp, Nunc) for 3 h at room temperature. On one plate, 2 molar equiv of 5 kDa NHS-PEG (0.75 nmol in 100 μL) was added and reacted with the bound albumin at 4 °C overnight. The albumin coating on the other plate was left unmodified to provide a control to differentiate between IgM binding to PEGylated and unmodified protein. Wells were washed 3 times with 200 μL of Tris buffered saline (TBS; 50 mM Tris-Cl, 150 mM NaCl, pH 7.5) containing 0.05% Tween-20 (wash buffer) and blocked with 200 μL of TBS containing 1% BSA for 1 h at room temperature. Wells were then washed 3 times with wash buffer. Plasma samples collected 7 d post sc or iv administration of trastuzumab or PEG–trastuzumab, or immediately before dosing (control plasma), were diluted 1:100 in TBS containing 1% BSA and 0.05% Tween-20 and added to the wells in duplicate (100 μL). Samples were incubated for 1 h at room temperature. Wells were then washed 5 times prior to the addition of goat anti-rat IgM-HRP conjugated antibody (100 μL, 1:10,000; Enzo Life Sciences) for 1 h at room temperature. The wells were then washed 5 times followed by the addition of o-phenylenediamine dihydrochloride solution (100 μL) for 30 min. Absorbance was measured at 450 nm using an EnSpire plate reader.

A second assay employing a dot blot was used to confirm the results of the ELISA-based anti-PEG IgM assay for rats administered PEG–trastuzumab. Briefly, 20 μL of 1:100 diluted plasma samples (predose and 7 days) were spotted onto a nitrocellulose membrane using a dot blot manifold. The membrane was left to dry before blocking with 5% BSA in TBS/Tween-20 for 1 h at room temperature on an orbital shaker. The membrane was then stained with goat anti-rat IgM-HRP (1:10000 in TBS/0.05% Tween-20 containing 0.1% BSA) for 1 h at room temperature. The membrane was washed 3 times (5 min) with TBS/Tween-20 prior to the addition of o-phenylenediamine dihydrochloride solution for detection and imaging. The intensity of the spots was then quantified using ImageJ software (version 1.48).

Permeability of PEG–Trastuzumab and Trastuzumab through HUVEC Monolayers. HUVEC monolayers were used to evaluate whether PEGylation impacts the permeability of trastuzumab through vascular epithelia. HUVECs were subcultured initially on 75 cm³ cell culture plates in EBM-2 culture media and were maintained at 37 °C in a humidified atmosphere and 5% CO_2. Cells were passaged via trypsin digestion, and 50,000 cells were seeded onto rat tail collagen (type I)-coated Transwell permeable support inserts (6.5 mm diameter, 0.33 cm²) on 24-well plates (Costar). Trans-endothelial electrical resistance (TEER) was measured every 3 days after seeding until a confluent monolayer was achieved (determined via a TEER > 66 Ω). This was usually between 15 and 21 d after seeding. Assessment of the baseline HUVEC monolayer integrity was conducted using ³H-mannitol. ³H-mannitol was added at a concentration of 1 μCi/mL, and trastuzumab and PEG–trastuzumab were added at a concentration of 8 μg/mL to either apical or basolateral layers. Permeability was measured in both apical to basolateral and basolateral to apical directions, and samples were collected at various time points over 24 h from either basal or apical chambers to enable measurement of flux profiles for mannitol, trastuzumab, and PEG–trastuzumab. Transendothelial flux was measured and the apparent permeability coefficient (P_{app}) calculated from $P_{app} = (dQ/dt)\cdot(1/(A\cdot C_0\cdot 60))$, where dQ/dt is the slope of the curve plotted for sample collected at different time points, A is the Transwell insert surface area, C_0 is the initial concentration in ng, and the factor of 60 is for conversion from minutes to seconds.

Statistical Analysis. The noncompartmental pharmacokinetic parameters for PEG–trastuzumab were compared to parameters for trastuzumab where possible via unpaired Student's t test. Plasma concentration−time profiles for iv and sc administered PEG–trastuzumab in control and lymph cannulated animals were compared over 30 h via two-way ANOVA with Bonferroni's test for significant differences at each time point. IgM levels after sc and iv administration of PEG–trastuzumab and trastuzumab were compared to predose plasma samples via one-way ANOVA with Tukey's post test. Significance was at a level of $p < 0.05$.

■ RESULTS

Preparation and Characterization of Mono-PEGylated Trastuzumab. The preparation of a mono-40 kDa PEG–trastuzumab was performed by conjugating a 40 kDa methoxy-PEG molecule to a lysine residue present on trastuzumab. In order to minimize steric interference of the PEG moiety with the antibody−antigen binding interaction site, precise equivalents of PEG were required to achieve the 1:1 molar ratio of PEG to trastuzumab. The synthesis and purification of the mono-PEGylated trastuzumab was confirmed by SDS−PAGE under reducing and nonreducing conditions, mass spectrometry, and SEC-MALS. The SDS−PAGE of the final PEGylated product and un-PEGylated trastuzumab is shown in Figure S1A (Supporting Information) and shows a single main band at

~150 kDa that corresponds to trastuzumab (nonreducing, lane 2) and at ~190 kDa (nonreducing, lane 3) that is consistent with mono-PEGylated trastuzumab. The SDS−PAGE with reducing gel conditions further confirmed the presence of the heavy and light chain species of PEG−trastuzumab, with the PEG attached onto the heavy chain (Figure S1A, lane 5, Supporting Information). Similarly, mass spectrometry of purified PEG−trastuzumab indicated that it was singly adducted, with a molecular weight of approximately 193 kDa (not shown).

The size and polydispersity of PEGylated and native trastuzumab were also examined via SEC-MALS. The average total molecular mass (Mw) of trastuzumab as determined by SEC-MALS was 147,000 ± 0.1% g/mol, consistent with the molecular weight calculated from the protein sequence (approximately 145 kDa). The polydispersity ratio of trastuzumab was 1.03, indicating a narrow mass distribution and no observable aggregates. The molar mass determined from the light scattering intensity using the concentration measured by differential refractive index for the PEGylated trastuzumab (190,000 ± 1.8% g/mol) and the absorbance at 280 nm for the protein component (148,000 ± 0.3% g/mol) are shown in Figure 1. The 148,000 g/mol mass of the protein
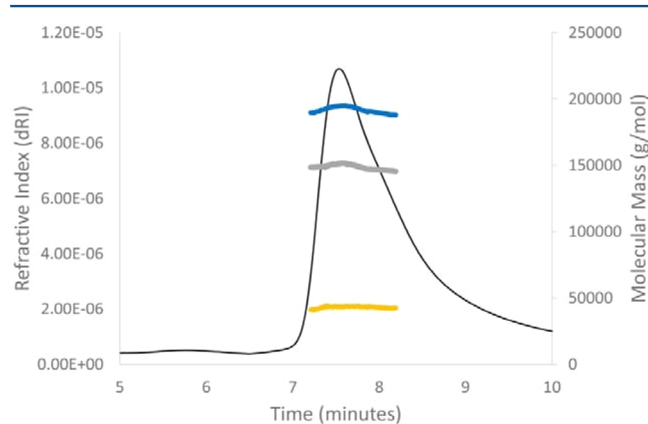
Figure 1. SEC-MALS analysis. PEG−trastuzumab was monitored by normalized differential refractive index (black line) and absorbance at 280 nm versus time. Molar mass was analyzed by multiangle light scattering following the total mass by differential refractive index (blue points), and protein mass by absorbance at 280 nm (gray points). The molar mass contributed by PEGylation is plotted as the difference between the total mass and the mass of the protein (orange points).

was consistent with the unmodified protein. The difference in the masses calculated from absorbance and refractive index (42,000 g/mol) can be attributed to PEGylation and is consistent with a singly adducted species.

MST analysis of the relative binding affinity of PEGylated and native trastuzumab (Figure 2) showed that trastuzumab binds HER2 with a K_D of 0.52 ± 0.07 nM consistent with data reported previously using surface plasmon resonance.[46] Following PEGylation, the affinity of trastuzumab for HER2 decreased by approximately 5-fold (K_D = 2.63 ± 0.46 nM; two tailed t test, p < 0.01).

***In Vitro* Growth Inhibitory Effects of Trastuzumab and PEG−Trastuzumab.** Trastuzumab and PEG−trastuzumab inhibited the growth of HER2 positive BT474 cells over 3 days in a concentration dependent manner (Figure 3). PEGylation did not have a significant impact on the growth inhibitory effects of trastuzumab over this time, and the
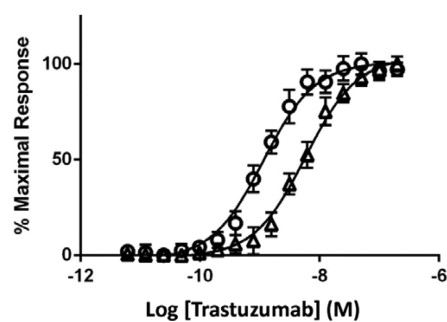
Figure 2. Binding of PEG−trastuzumab (△) and trastuzumab (○) to HER2. Values on the Y-axis represent the percentage of the maximal thermophoretic response (MST) observed. Inset shows raw data. All binding curves were determined in triplicate by MST and are represented as the mean ± SD.

calculated IC_{50} values were 0.11 μg/mL for trastuzumab and 0.12 μg/mL for PEG−trastuzumab. Neither trastuzumab nor PEG−trastuzumab inhibited the growth of HER2 negative T47D cells (not shown).

Cellular Trafficking of PEG−Trastuzumab in BT474 Cells. Trastuzumab and PEG−trastuzumab were fluorescently labeled with Alexa488 (Figures S1B and S1C, Supporting Information) to investigate how PEGylation influences cellular HER2 binding and intracellular trafficking of the antibody in BT474 cells. Figures 4A and 4D show control staining of early endosomes and nuclei. Binding of both Alexa488-labeled PEG−trastuzumab and trastuzumab to the plasma membrane of BT474 cells was observed within 3 h after the addition of antibody to cells (not shown). Evidence of some cellular internalization was seen after 24 h (not shown), but was more pronounced after 48 h (Figures 4B and 4C). Early endosomes were present within cells incubated with trastuzumab and PEG−trastuzumab at 48 h, but colocalization of Alexa488-trastuzumab with these endosomes was sparse (Figure 4B,E,G). On the other hand, colocalization of Alexa488-PEG−trastuzumab within early endosomes was more prominent after 48 h when compared to Alexa488-trastuzumab (Figure 4C,F,H).

Noncompartmental Pharmacokinetics of PEG−Trastuzumab after Iv and Sc Administration in Rats. Following iv administration of PEG−trastuzumab to non lymph cannulated rats, plasma concentrations declined with a terminal half-life of 169 ± 47.3 h (Figure 5, Table 1). In contrast, the terminal half-life of PEG−trastuzumab after sc administration was significantly shorter (36.9 ± 1.96 h). In these animals, a sharp decline in PEG−trastuzumab plasma concentrations was observed after approximately 7 days, which was not seen previously in rats administered trastuzumab sc (Figure 5), suggesting the potential for production of anti-PEG antibodies in response to sc PEG−trastuzumab.

The noncompartmental values for T_{max}, C_{max}, and $t_{1/2}$ after iv administration of PEG−trastuzumab were not significantly different from those of trastuzumab (unpaired t test; Table 1). The area under the plasma concentration−time curve ($AUC_{0−\infty}$) after sc administration of PEG−trastuzumab was significantly lower (2026 mg·h/L) when compared to trastuzumab (6401 mg·h/L).[10] The continuous removal of lymph from the thoracic lymph duct cannula in rats administered PEG−trastuzumab iv or sc led to a significant reduction in plasma concentrations at later time points when compared to non lymph cannulated rats (Figure S2, Supporting
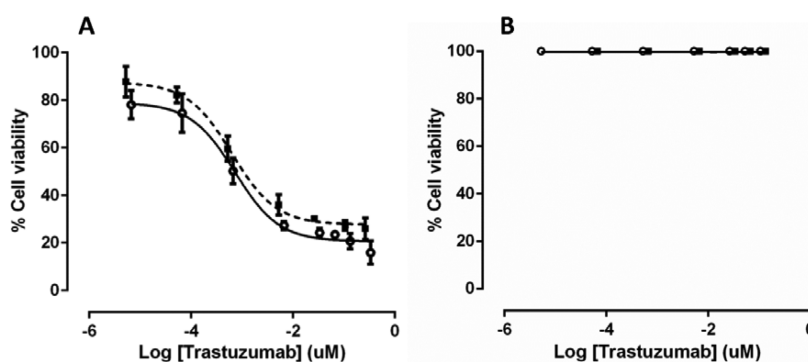
Figure 3. *In vitro* growth inhibition of (A) BT474 human breast cancer cells and (B) T47D cells by PEG−trastuzumab (■) and trastuzumab (○). Growth inhibition curves were fitted using a sigmoidal dose−response (inhibition) curve on GraphPad Prism. Values are expressed as mean ± SD (n = 3).
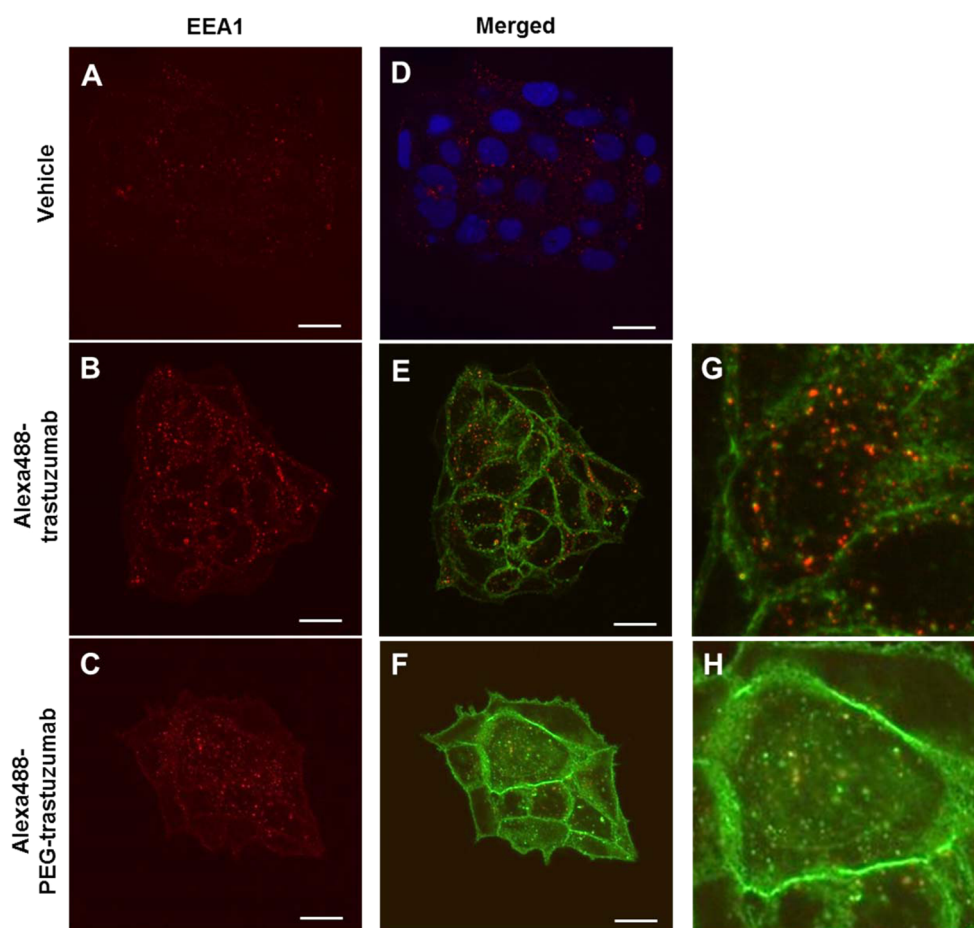
Figure 4. Confocal fluorescence microscopy (60× magnification) showing cell surface binding and colocalization of trastuzumab and PEG−trastuzumab with early endosomes (EEA1) in BT474 cells after a 48 h incubation. (A) EEA1 staining (red) alone, (B) EEA1 staining (red) in the presence of 1 μg/mL Alexa488-trastuzumab (green), and (C) EEA1 staining (red) in the presence of 1 μg/mL Alexa488-PEG−trastuzumab (green). (D) Merged images of BT474 EEA1 (red) and nuclei stain with SYTO40 blue. Merged images (orange) of EEA1 (red) and (E) Alexa488-trastuzumab and (F) Alexa488-PEG−trastuzumab (green). Enlarged images from E and F of either (G) trastuzumab or (H) PEG−trastuzumab uptake into early endosomes. Scale bar indicates 20 μm.

Information). As a result, AUC_{0-30h} in lymph cannulated rats was significantly reduced after iv and sc administration when compared to non lymph cannulated rats (Table 1). The recovery of PEG−trastuzumab in lymph collected over 30 h was 38.5 ± 6.19% of the dose after iv administration and 29.4 ± 9.49% of dose after sc administration in lymph cannulated rats and did not differ significantly from the proportion of trastuzumab recovered in lymph.

Population Pharmacokinetics of PEG−Trastuzumab after Iv and Sc Administration in Rats. The refined PK model contained eight compartments and simultaneously fitted all PEG−trastuzumab and trastuzumab plasma concentrations and the amounts recovered in lymph. In comparison to previous models,[10,40] the refined model for PEG−trastuzumab and trastuzumab (Figure 6) did not include drug transfer from the peripheral compartment to the peripheral lymph compart-

G

Intravenous dosing

Subcutaneous dosing
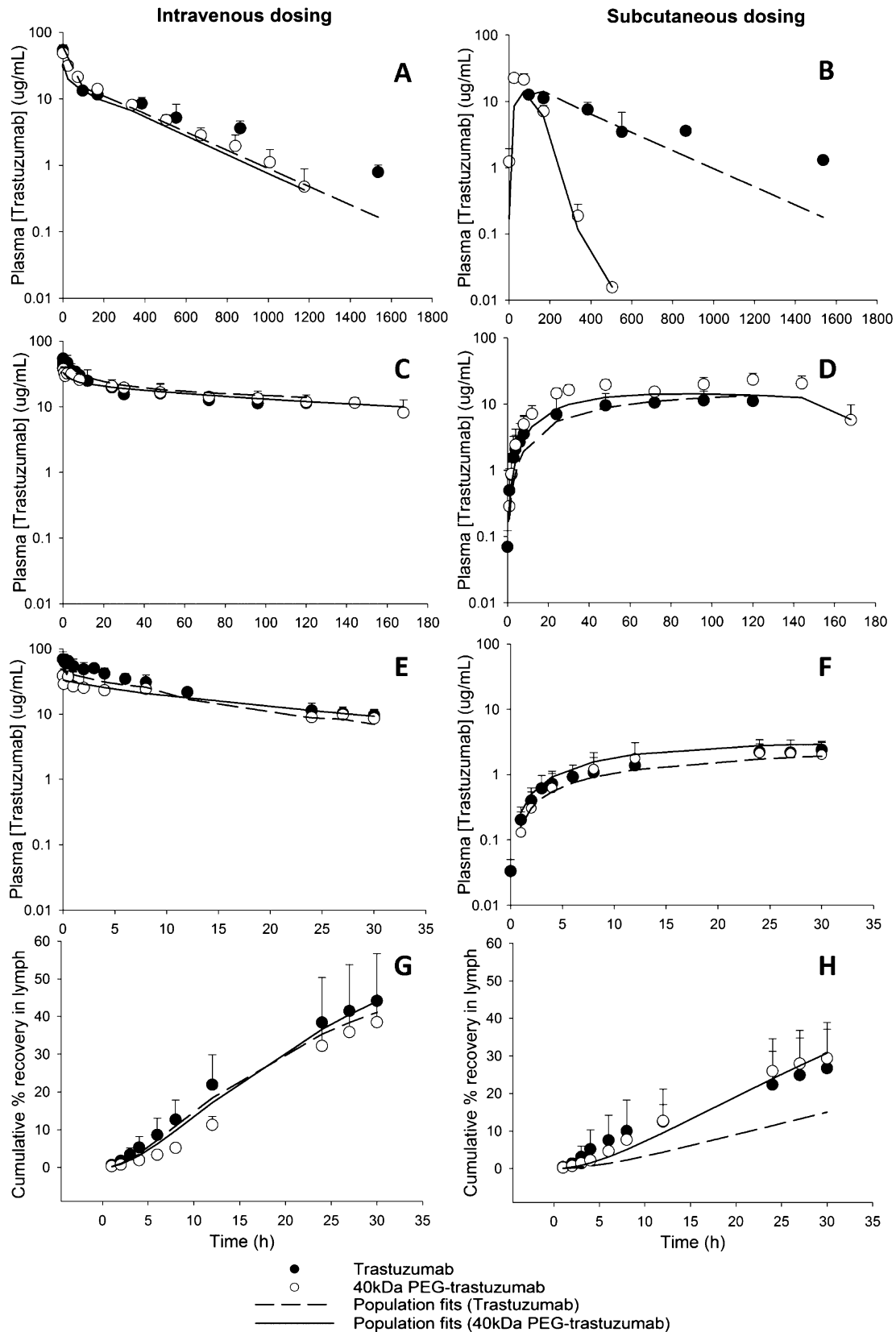
Figure 5. Iv and sc plasma concentration−time profiles of PEG−trastuzumab in control and thoracic lymph duct-cannulated rats dosed at 2 mg/kg. (A, B) Plasma profiles of long-term control rats (49 d) without cannulations after iv and sc dosing. (C, D) Plasma profiles of short-term control rats (7 d) with jugular and/or carotid cannulations. (E, F) Plasma profiles of thoracic lymph duct-cannulated rats (30 h). (G, H) Cumulative lymph profiles of thoracic lymph duct-cannulated rats (30 h). Data is represented as mean ± SD (n = 4−5). Data for trastuzumab was reproduced from a previous study.[10]

Table 1. Noncompartmental Pharmacokinetic Parameters for PEG–Trastuzumab and Trastzumab[a]

param[b]	unit	PEG–trastuzumab				trastuzumab			
				lymph cannulated				lymph cannulated	
		iv	sc	iv	sc	iv	sc	iv	sc
T_{max}	h		110 ± 36.4		23.3 ± 7.89^c		75.4 ± 16.6		28.5 ± 3.00
C_{max}	mg/L		17.9 ± 9.73		2.04 ± 1.24^c		11.1 ± 4.58		2.39 ± 0.727
$t_{1/2}$	h	169 ± 47.3	36.9 ± 1.96			285 ± 111	262 ± 200		
AUC_{0-30h}	mg/L·h	632 ± 40.9	177 ± 79.1	529 ± 33.5	41.6 ± 29.3	776 ± 193	143 ± 112	700 ± 133	44.9 ± 17.9
$AUC_{0-\infty}$	mg/L·h	4041^d	2026^d			8188	6401		
CL	mL/h	$0.135,^d$ 0.124 median	$0.344,^d$ 0.199 median			0.0720	0.0922		
F_{lymph}	%			38.5 ± 6.19	29.4 ± 9.49			44.7 ± 12.9	27.0 ± 10.4

[a]Data for trastuzumab was reproduced from a previous study.[10] [b]C_{max}: observed peak concentration. T_{max}: time of C_{max}. $t_{1/2}$: terminal half-life. AUC_{0-30h}: area under the plasma concentration time curve from time 0 to 30 h. $AUC_{0-\infty}$: area under the plasma concentration time curve from time 0 h to infinity. F_{lymph}: fraction of dose recovered in lymph between 0 and 30 h. CL: total body clearance. [c]Last lymph collection period was limited to 30 h by animal ethics and practical requirements. [d]As data from rats sampled over 120 h and long-term rats sampled over two months were used to obtain this estimate, calculation of a standard deviation by noncompartmental methods is not directly possible. Instead, a population PK modeling analysis was performed.
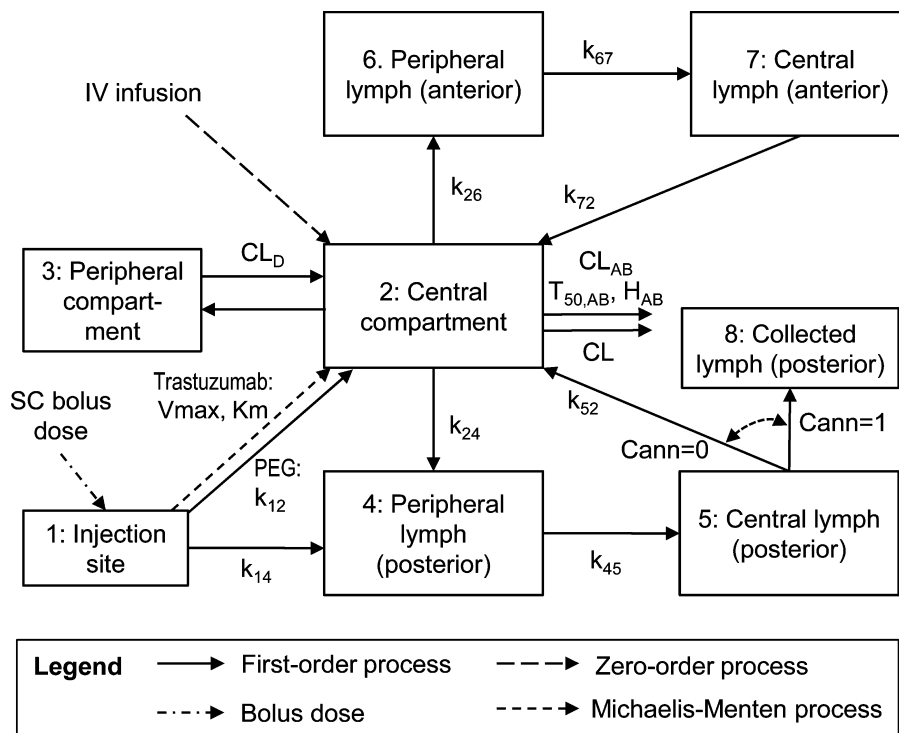
Figure 6. Structure of the mechanism-based model for PEG–trastuzumab and trastuzumab in rats. Absorption from the injection site to the central compartment followed Michaelis–Menten kinetics for trastuzumab and first-order kinetics for PEG–trastuzumab.

ments as it yielded no benefit during a simultaneous analysis of all PEG–trastuzumab and trastuzumab data. Therefore, the first-order rate constants (k_{34} and k_{36}) were set to zero. Individual and population fits were reasonably unbiased and precise for plasma concentrations and the fractions of dose collected in lymph (Figure 5 and Figure S3, Supporting Information). The population fitted cumulative fractions of drug collected in lymph matched the observations well for PEG–trastuzumab after sc dosing and trastuzumab after iv dosing. However, some misfits were apparent for trastuzumab after sc dosing. The individual curve fits for these lymph excretion profiles matched the observations more closely as shown in the Supporting Information provided (Figure S3, Supporting Information). The model appropriately captured the rapid decline in the plasma concentrations for PEG–

trastuzumab after sc dosing, however the predicted amounts of trastuzumab in lymph were smaller than the observed fractions during the first 8 h (Figure 5) for sc dosing.

For PEG–trastuzumab, absorption was best described by first-order processes from the sc injection site into the central compartment (mean transit time: 120 h) and posterior peripheral lymph compartment (mean transit time: 70.2 h). In contrast, for trastuzumab, absorption from the sc injection site was best described by a Michaelis–Menten process into the central compartment and a first-order process into the posterior peripheral lymph compartment. The estimated absolute bioavailability of PEG–trastuzumab after sc dosing was above 99.9% and was eventually fixed to 100%. Absolute bioavailability was estimated as 86.1% for trastuzumab. The volume of distribution at steady state (i.e., the sum of V_1 and V_2) was

Table 2. Estimated Population Pharmacokinetic Model Parameters for PEG–Trastuzumab and Trastuzumab[a]

param	symbol	unit	PEG–trastuzumab		trastuzumab	
			population mean (SE)	between subject variability (SE)	population mean (SE)	between subject variability (SE)
bioavailability[b] for sc dosing	F		1 (fixed)		0.861 (8.3%)	$[0.856-0.867]^c$
vol of distribution of central compartment	V_1	mL	15.1 (2.5%)	0.0703 (112%)[d]	9.85 (9.5%)	0.335 (125%)[d]
vol of distribution of peripheral compartment	V_2	mL	6.15 (6%)	0.0511 (183%)	12.2 (23%)	0.806 (53%)
clearance	CL	mL/h	0.0860 (15%)	0.338 (86%)	0.0821 (15%)	0.345 (69%)
distribution clearance	CLd	mL/h	0.0764 (22%)	0.118 (332%)	0.360 (22%)	0.228 (94%)
clearance due to an immune-mediate elimination	CL_{AB}	mL/h	1.42 (45%)	0.451 (183%)	e	
time of 50% onset of immune mediated clearance	$T_{50,AB}$	d	6.61 (2.2%)	0.038 (236%)	e	
Hill coefficient for onset of immune mediate clearance	H_{AB}		30 (fixed)		e	
maximum rate of absorption from sc injection site to the central compartment	Vmax$_{12}$	μg/h			1.69 (36%)	1.07 (86%)
amount of absorption from sc injection site to the central compartment	Km$_{12}$	μg			0.639 (87%)	0.495 (253%)
MTT[f] from the sc injection site to the central compartment	MTT$_{12}$[g,h]	h	120 (26%)	1.51 (44%)		
MTT from the sc injection site to posterior peripheral lymph	MTT$_{14}$[g,h]	h	70.2 (15%)	0.318 (118%)	139 (25%)	0.723 (80%)
MTT from central compartment to peripheral lymph	MTT$_{24}$[g,h]	h	30.7 (1.9%)	0.0201 (325%)	24.2 (18%)	0.275 (110%)
MTT from peripheral lymph to central lymph	MTT$_{45}$[g,h]	h	2.85 (64%)[i]	0.320 (297%)	2.85 (64%)[i]	0.320 (297%)
	MTT$_{45,cannulated}$[g,h]	h	5.65 (24%)[i]	1.18 (28%)	5.65 (24%)[i]	1.18 (28%)
MTT from central lymph to central compartment	MTT$_{52}$	min	10 (fixed)		10 (fixed)	
SD of additive residual error for plasma concentrations	SDin	mg/L	0.0657 (15%)		0.0657 (15%)	
SD of proportional residual error for plasma concentrations	SDsl		0.140 (4.3%)		0.140 (4.3%)	
SD of additive residual error for fraction of dose eliminated in lymph	LDin	fraction of dose (%)	0.664 (9.1%)		0.664 (9.1%)	
SD of proportional residual error for fraction of dose eliminated in lymph	LDsl		0.120 (31%)		0.168 (18%)	

[a]Data for trastuzumab was reproduced from a previous study.[10] [b]Bioavailability was estimated as a logistically transformed parameter to constrain the individual estimates between 0 and 100%. On logistically transformed scale, the population mean of $F_{transformed}$ was 1.83 and the SD on transformed scale was 0.242. [c]Range of individual estimates. [d]The estimate represents the apparent coefficient of variation of a normal distribution on natural log-scale, and the estimate in parentheses is the relative standard error of the estimated variance on natural log-scale. [e]Process not part of the model for the respective compound. [f]Mean transit time. [g]The mean transit times were estimated via modeling. The rate constants shown in Figure 6 were calculated as the inverse of these mean transit times. [h]Assuming that the distributions to the anterior and posterior lymph loops were comparably fast, k_{26} was fixed to the estimate of k_{24}, k_{67} was fixed to the estimate of k_{45}, and k_{72} was fixed to the value of k_{52}. [i]Modeling estimated that the transfer from peripheral to central lymph was slightly slower ($p < 0.01$, likelihood ratio test) for cannulated rats compared to the long-term noncannulated rats. Given the much slower rate of drug transfer to the peripheral lymph compartment, the difference between MTT$_{45}$ and MTT$_{45,cannulated}$ only had a small overall impact on the lymph profiles.

comparable between PEG–trastuzumab and trastuzumab. However, PEG–trastuzumab had a larger V_1 compared to trastuzumab, suggesting that PEG–trastuzumab did not penetrate as extensively into the peripheral compartment (i.e., compartment 3, Figure 5).

The first-order elimination clearances were small and similar for PEG–trastuzumab and trastuzumab (Table 2). Inclusion of a Michaelis–Menten clearance from the central compartment neither improved the objective function nor the curve fits. After sc dosing of PEG–trastuzumab, an additional rapid clearance (1.42 mL/h) was visible which started after approximately 6 days ($T_{50,AB}$, Table 2; Figure 5). This additional clearance was hypothesized to be mediated by an immune response and was not present after iv dosing of PEG–trastuzumab. We utilized a Hill function to describe the change in the proposed "immune" related clearance over time $[CL_{AB}(t)]$:

$$CL_{AB}(t) = \frac{time^{H_{AB}}}{time^{H_{AB}} + T_{50,AB}^{H_{AB}}} \cdot CL_{AB}$$

The CL_{AB} is the maximum "immune" related clearance at full induction, $T_{50,AB}$ the time to 50% induction, and H_{AB} the Hill coefficient. The onset of the "immune" related clearance occurred over a short time. We therefore fixed H_{AB} to 30, which represents a rapid increase of $CL_{AB}(t)$ from 5% of CL_{AB} at 6.0 d to 95% of CL_{AB} at 7.3 d.

Based on the final model (Figure 6) and parameter estimates (Table 2), we then simulated the time course of antibody concentrations in plasma and lymph. The simulation predicted that peak concentrations of PEG–trastuzumab in the peripheral lymph were higher compared to trastuzumab, although the raw data show no significant differences in lymphatic exposure after sc administration (Figure 5). After approximately 7 days (Table 2), the model predicted a sharp decline of PEG–trastuzumab in lymph and plasma due to the potential generation of anti-PEG antibodies compared to a slow first-order decrease of trastuzumab up to 28 days (Figure 5).

The simulated fraction of the PEG–trastuzumab dose flowing through the posterior lymph loop up to 28 days post administration was 284% for sc dosing and 570% for iv dosing in non lymph cannulated rats and 468% (sc) to 496% (iv) for

trastuzumab (Table 3). This indicated that PEG-trastuzumab transitioned on average between 2.8 and 5.7 times through the

Table 3. Predicted Fractions of Administered Dose Flowing through the Posterior and Anterior Lymph Loops between Time Zero and Infinity after Iv or Sc Dosing of 2 mg/kg PEG−Trastuzumab and Trastuzumab with and without Thoracic Lymph Duct Cannulation[a]

			fraction of dose flowing through lymph loop, %	
PEG	cannulated	route	posterior	anterior
yes	no	sc	284[b,c]	221[b,c]
yes	no	iv	570[b]	570[b]
yes	yes	sc	91.8[d]	28.6[d]
yes	yes	iv	85.1[d]	85.1[d]
no	no	sc	468[b]	427[b]
no	no	iv	496[b]	496[b]
no	yes	sc	78.5[d]	37.9[d]
no	yes	iv	83.2[d]	83.2[d]

[a]Data for trastuzumab was reproduced from a previous study.[10] [b]These estimates mean that, on average, an antibody molecule flows through the respective lymph loop approximately 4 to 5 times for trastuzumab and 2 to 6 times for PEG−trastuzumab before the molecule is eliminated. This is conceivable given the long terminal half-life and extensive distribution of trastuzumab in lymph. [c]These simulated fractions are smaller than those after intravenous dosing of PEG−trastuzumab due to the presence of the antibody mediated clearance which was only part of the model for sc dosing of PEG−trastuzumab. [d]As lymph from the posterior loop is quantitatively sampled in cannulated animals, these fractions were considerably lower, as expected.

posterior lymph before it was eliminated. The rapid "immune" related clearance caused this fraction to be lower after sc dosing for PEG−trastuzumab compared to trastuzumab. As antibody is absorbed directly from the sc injection site into the posterior lymph compartment (i.e., targeted delivery), the model predicted fractions of dose were higher in the posterior lymph compartment compared to the anterior side (Figure 7, Table 3).

Determination of Anti-PEG IgM Antibody Production after Iv and Sc Administration of PEG−Trastuzumab and Trastuzumab. In order to evaluate whether the increase in PEG−trastuzumab plasma clearance 7 days after sc administration was a result of a localized immune reaction at the injection site that led to the production of anti-PEG IgM, we measured the levels of anti-PEG IgM in plasma collected 7 days after administration of PEG−trastuzumab via iv and sc routes using a well-documented ELISA method. This was compared to the results in rats administered native trastuzumab. None of the plasma samples collected from rats administered PEG−trastuzumab or trastuzumab showed a significant increase in optical absorbance when compared to blank plasma in plates coated with only BSA (Figure 8A). In addition, absorbance values from the plasma of rats administered PEG−trastuzumab via the iv route, or trastuzumab via sc or iv routes, did not differ significantly when compared to plasma collected from the same rats prior to antibody administration on plates coated with PEGylated BSA. The plasma from rats administered sc PEG−trastuzumab, however, showed a positive reaction for anti-PEG IgM, and absorbance values were approximately 4-fold higher for sc dosed rats when compared to predose plasma (Figure 8B). Interestingly, when wells were coated with 1,2-distearoyl-
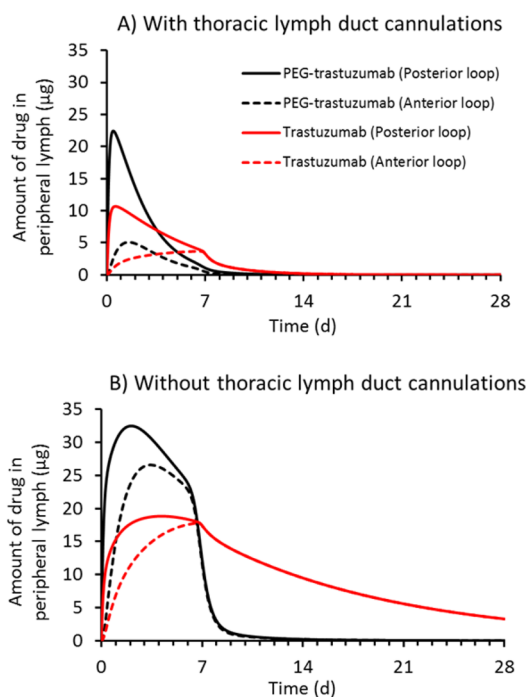
Figure 7. Simulated typical amounts PEG−trastuzumab and trastuzumab in the posterior and anterior peripheral lymph in (A) thoracic lymph duct cannulated and (B) nonthoracic lymph duct cannulated rats after sc administration of 2 mg/kg. Data for trastuzumab was reproduced from a previous study.[10]

sn-glycero-3-phosphoethanolamine-N-methoxy(PEG)-2000 (PEG$_{2000}$-DSPE) according to a previous method,[45] anti-PEG IgM was not detected, suggesting that the anti-PEG IgM produced was specific for PEGylated proteins, and not the PEG alone (data not shown).

These observations in the plasma of rats administered PEG−trastuzumab were also confirmed using a dot blot assay which involves the initial retention of all proteins present in plasma on a nitrocellulose membrane prior to antibody detection of total rat IgM. The dot blot assay confirmed the increased production of total IgM following sc administration of PEG−trastuzumab (Figure S4, Supporting Information).

Permeability of PEG−Trastuzumab and Trastuzumab through HUVEC Monolayers. To better understand the impact of PEGylation on the vascular permeability and trafficking of trastuzumab, the permeability of PEG−trastuzumab and trastuzumab through confluent HUVEC monolayers was investigated in the apical to basolateral and basolateral to apical directions. The integrity of the HUVEC monolayer over the time course of the study was confirmed via ^{3}H-mannitol. Permeability coefficient values (P_{app}) obtained for ^{3}H-mannitol from both apical and basal acceptor chambers were similar where the efflux ratio = 1 (Table S5, Supporting Information), indicating nonpolarized transport through the HUVEC monolayer. Conversely, P_{app} values obtained for both PEG−trastuzumab and trastuzumab were much lower compared to ^{3}H-mannitol, suggesting slower permeability for the macromolecules. The P_{app} value for PEG−trastuzumab was not significantly different from that for trastuzumab in the apical to basolateral direction, but was approximately 4-fold lower in the basolateral to apical direction, suggesting slower vascular permeability from the subcutaneous injection site into blood (Table S5, Supporting Information).
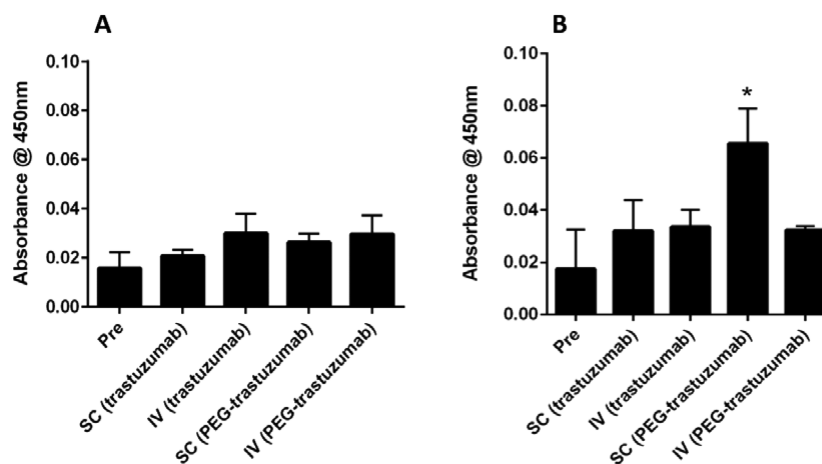
Figure 8. Semiquantitative production of anti-PEG IgM 7 d after sc or iv administration of PEG−trastuzumab or trastuzumab. (A) Absorbance values from a control plate coated with albumin alone (nonPEGylated). (B) Absorbance values from a plate coated with PEGylated albumin. Pre values represent absorbance from plasma collected prior to iv or sc dosing of the antibody. Values are expressed as mean ± SD ($n = 3$). *$p < 0.05$ cf. pre sample and iv PEG−trastuzumab.

■ DISCUSSION

The main objective of this study was to explore the impact of PEGylation on the sc pharmacokinetics and lymphatic disposition of trastuzumab after iv and sc administration to rats. To further understand the biological effects of PEGylation, *in vitro* experiments were conducted to determine the HER2 receptor binding kinetics of PEG−trastuzumab, its ability to inhibit cancer cell proliferation, and cellular trafficking profile.

PEGylation strategies have been commonly employed to prolong drug and macromolecule residence times within the systemic circulation and, as a result, to improve *in vivo* biological/therapeutic activity. PEGylation also has the potential to improve the subcutaneous bioavailability and lymphatic disposition of therapeutic proteins and drug delivery systems via various mechanisms.[12,13] More recently, the concept of targeted drug delivery to the lymphatic system for the treatment of lymph-resident cancers has emerged and is increasingly being employed for the development of therapeutics for lymphatic and lymph-metastatic cancers. To date, however, the impact of PEGylation on the pharmaceutical behavior of very large proteins such as antibodies has not been described in detail. To our knowledge, this is the first report to describe the effect of PEGylation on the subcutaneous pharmacokinetics and lymphatic disposition of a mAb, using the chemotherapeutic human mAb trastuzumab as a model. In this instance, trastuzumab was mono-PEGylated with 40 kDa linear PEG to give a product with approximately 20% w/w PEG loading. This was expected to increase the hydrophilicity and aqueous solubility of the mAb, without dramatically altering molecular weight or *in vitro* activity/receptor binding, thus enabling a more defined evaluation of the effect of conjugation of the highly water-soluble "stealth" polymer on *in vivo* and *in vitro* trafficking and disposition.

Despite minimal PEG loading, a 5-fold decrease in the HER2 binding affinity of PEG−trastuzumab was observed compared to native trastuzumab. Since the reaction was performed via nonspecific conjugation of PEG to lysine groups within the trastuzumab structure, a statistical mixture of adduction sites was expected. The current data suggest that the sites of conjugation may have included attachment to (or interference with) the antigen binding domain, thereby hindering HER2 recognition by the large 40 kDa PEG.

Nevertheless, PEG−trastuzumab displayed equivalent growth inhibition to native trastuzumab in BT474 cells, suggesting that the presence of PEG may have altered cellular trafficking or stability of the mAb *in vitro*. We therefore sought to further understand the mechanisms of PEG−trastuzumab and trastuzumab cellular trafficking. The results demonstrated the binding of both PEG−trastuzumab and trastuzumab to HER2 receptors expressed on the surface of BT474 cells. While the majority of PEGylated and native trastuzumab was found to remain within or close to the plasma membrane after 48 h, early endosome formation and colocalization with trastuzumab and PEG−trastuzumab can be seen within the cells. Colocalization between trastuzumab and early endosomes was relatively sparse after 48 h. However, PEG−trastuzumab binding to the plasma membrane appeared to be more evident when compared to trastuzumab and colocalization of PEG−trastuzumab with the early endosomes also appeared to be more prominent. This was interesting given that PEG loading typically limits the cellular uptake of macromolecules.[47] It is therefore possible that, despite reduced affinity of PEG−trastuzumab for HER2, the presence of the PEG may change the cellular trafficking and cell surface interaction of trastuzumab such that the growth inhibitory effect of the antibody is preserved. This suggests that improvements in the pharmaceutical behavior, tumor, or lymphatic disposition of trastuzumab as a result of PEGylation may translate into improved therapeutic outcomes.

Intracellular FcRn receptors are also important in protecting antibodies from enzyme-mediated degradation and in recycling the antibodies to the cell surface.[48,49] While this study did not specifically examine the binding affinity of PEG−trastuzumab with FcRn receptors, we expect that it would be reduced when compared to native trastuzumab as observed for HER2. This suggests that PEGylated trastuzumab might display increased intracellular degradation when compared to trastuzumab, although conversely, the PEG moiety may also protect the antibody against intracellular degradation as described for other PEGylated proteins.[33,50] In addition, reduced binding to intracellular FcRn receptors may also promote enhanced intracellular retention as a result of reduced recycling of the antibody to the cell surface.[51] This is consistent with our cellular transport studies showing better colocalization of

PEG−trastuzumab with early endosomes when compared to native trastuzumab.

Although the precise mechanism of PEG−trastuzumab and trastuzumab cellular activity remains unclear, several mechanisms have been proposed to explain the cellular activity and trafficking of the mAb. To date, the proposed mechanisms of action for trastuzumab include the prevention of HER2 dimerization or shedding of the extracellular domain, resulting in decreased signaling[52] and a reduction in HER2 expression at the cell surface by increasing endosomal/lysosomal destruction of the receptor.[53−55] Conversely, others have suggested that the majority of trastuzumab remains bound to HER2 and does not get internalized or recycled.[46,56]

To describe changes in the pharmacokinetic behavior of trastuzumab in rats following PEGylation, a population pharmacokinetic model was developed and refined based on our previously published models[10,40] to simultaneously describe and predict PEG−trastuzumab and trastuzumab concentrations in plasma and lymph. This modeling approach enabled prediction of the time-course of lymph and plasma concentrations after sc and iv dosing with and without thoracic lymph duct cannulation, over longer time periods than those that were observable over the limited time course (30 h) in lymph cannulated rats. Our population model additionally accounts for between animal variability and for drug absorption from the sc injection site, as well as from the central compartment into peripheral lymph.

The data showed that after iv administration, the plasma and lymphatic pharmacokinetics of PEG−trastuzumab and trastuzumab were similar. This was in contrast to the results of a previous study by Deckert et al. that examined the iv pharmacokinetics of a humanized A33 antibody in mice. In this study, PEGylation of the A33 antibody resulted in an increase in the terminal half-life when compared to the native antibody.[30] This may have been due to the fact that PEGylation of the A33 antibody was performed by conjugating multiple (15 to 30) smaller molecular weight PEGs (5000−20000 Da) to a single antibody (final PEG to antibody ratios used were 15:1 PEG_{20000} to antibody and 30:1 PEG_{5000} to antibody). In addition, differential binding kinetics between PEGylated and native trastuzumab with soluble HER2 in plasma may play a role in the pharmacokinetic behavior of trastuzumab.[57]

The initial plasma pharmacokinetics of PEG−trastuzumab was similar to that of trastuzumab after sc administration, although in vitro P_{app} values suggested slower basolateral to apical vascular permeability for PEG−trastuzumab, suggesting slower vascular absorption from an sc injection site. This suggests that the presence of the PEG may have increased convection of trastuzumab from the sc injection site which would offset any reductions in vascular permeability as previously described,[58,59] although at this point it is unclear whether the reduced vascular permeability was a result of slowed paracellular or transcellular transport. In stark contrast to native trastuzumab, however, PEG−trastuzumab displayed a significantly shorter terminal half-life after sc administration. The sharp decline in plasma concentrations of PEG−trastuzumab was observed approximately 7 days after sc administration of 2 mg/kg to rats. This was evident in both short-term and long-term sc dosed rats, and plasma levels of PEG−trastuzumab were below the level of accurate quantification after 21 days.

Previous animal studies have shown that certain PEGylated proteins can elicit an immune response that is directed to the PEG-conjugated protein, in contrast to the typical assertion that PEG is nonimmunogenic.[60,61] A study by Sherman et al., for instance, demonstrated that the conjugation of methoxy-PEG to three dissimilar proteins which contained as few as 1 or as many as 17 PEG molecules resulted in the generation of anti-PEG antibodies against the methoxy group.[61] Armstrong et al. also identified that the production of anti-PEG antibodies was responsible for the accelerated clearance of methoxy-PEG conjugates of asparaginase in a subset of human patients.[62] Initial doses of some PEGylated colloids have also been demonstrated to induce the production of anti-PEG IgM, which was responsible for the accelerated plasma clearance of subsequent doses of colloid in various species. The effect was also highly dependent on the initial dose given.[45] It is perhaps not surprising, therefore, that we identified anti-PEG IgM in the plasma of rats administered 2 mg/kg PEG−trastuzumab at 7 days which presumably stimulated the late-onset rapid clearance of PEG−trastuzumab from plasma. It was interesting that a similar response was not observed in iv dosed rats, and this suggests that sc administration led to increased exposure of PEG−trastuzumab to antigen presenting cells at the injection site (or in the draining lymph nodes) and a more rapid production of anti-PEG IgM. This is consistent with the vaccine literature that suggests that interstitial administration of antigens results in more rapid and pronounced immunity when compared to iv administration.[16] This does not discount the possibility that PEG−trastuzumab might not elicit this response in humans, since it is possible that the administration of a human derived monoclonal antibody to rats may have enhanced the immune response against the PEGylated protein. In support of this suggestion, our preliminary observations with a 40 kDa PEG-conjugated Fab fragment of trastuzumab did not show an accelerated plasma clearance in sc dosed rats after 7 days, suggesting that the Fc portion of trastuzumab may have played a role in stimulating the immune response observed here (unpublished data).

Despite the accelerated clearance of PEG−trastuzumab after sc administration, PEGylation also improved the bioavailability of trastuzumab, leading to complete absorption (in contrast to approximately 86% absorption for trastuzumab). This lends further support to the suggestion that PEGylation improved convection away from the injection site through interstitial water channels.

The data revealed that exposure of central lymph to PEG−trastuzumab and trastuzumab did not differ significantly after sc or iv administration, although the model predicted 2-fold more rapid transport of PEG−trastuzumab into peripheral lymph when compared to trastuzumab. The presence of PEG−trastuzumab in the thoracic lymph after iv administration reflects extravasation from the capillary beds into the lymphatics, indicating the importance of the lymphatic system in the disposition of PEG−trastuzumab as shown previously for trastuzumab in rats.[10] This is supported by simulation results predicting that, on average (for non lymph cannulated rats), an antibody molecule flows through each lymph loop (posterior and anterior) approximately 2 to 6 times for PEG−trastuzumab and 4 to 5 times for trastuzumab[10] before being eliminated.

Increasing the molecular size of drug molecules is known to increase drainage into the lymph from the injection site.[24] To date, the largest protein that has been studied for lymphatic uptake is a 84 kDa protein that was administered subcutaneously to sheep.[63] This protein showed almost complete absorption entirely via the lymph. Large proteins within the

range of 30 to 40 kDa were also found to have similar maximal absorption through the peripheral lymphatics in sheep.[64,65] Many of these studies have investigated lymphatic uptake into peripheral lymph after injection into the interdigital space, which is under very high interstitial pressure that likely promotes more rapid and extensive lymphatic uptake. Lymphatic transport studies of this nature in sheep have therefore shown much higher lymphatic uptake when compared to sc administration in rats.[21] While the nanoparticle literature shows that particle sizes in excess of approximately 100 nm display restricted convection away from the sc injection site[66] and, as a result, reduced lymphatic transport and bioavailability, the data for trastuzumab and PEG−trastuzumab suggest that lymphatic transport is unlikely to be impeded for very large ~150 kDa proteins. Variations in lymphatic function and transport should therefore be considered as probable factors that can contribute to the variable pharmacokinetics of therapeutic proteins. This is especially important for the treatment of critically ill patients who are predominantly bedridden and immobile.

In conclusion, this study showed that the initial plasma and lymphatic pharmacokinetics of PEG−trastuzumab after sc and iv administration were similar to that of the native protein. The data suggest that while PEGylation appears to restrict basolateral to apical vascular transport, convection of the protein from the sc injection site likely contributes to maintaining efficient *in vivo* vascular absorption and enhanced bioavailability, although this requires further investigation. However, an accelerated plasma clearance was observed for PEG−trastuzumab after approximately 7 days in sc dosed animals, and the data suggested that this was likely to have been a result of the production of IgM antibodies against PEGylated protein as others have observed in animal models and human subjects. While the binding affinity of PEG−trastuzumab was approximately 5-fold lower than that of trastuzumab, cell-based studies suggest that PEG−trastuzumab displays different cellular trafficking properties that contribute to maintaining comparable growth inhibition effects against HER2 over-expressing breast cancer cells *in vitro*. The data therefore suggest that, in the clinical setting, there is unlikely to be a therapeutic benefit to the PEGylation of very large proteins such as mAbs, since the plasma and lymphatic pharmacokinetics and cellular activity of PEGylated and native trastuzumab were similar. The presence of the PEG moiety, however, may stimulate an immunological response against the PEGylated protein, leading to increased clearance and, ultimately, reduced therapeutic activity. In contrast, however, previous work suggests that there is scope to improve the lymphatic exposure and *in vivo* chemotherapeutic activity of smaller antibody fragments, such as therapeutic fragment antigen-binding (Fabs) or nanobodies, which will be the subject of further work.

ASSOCIATED CONTENT

Ⓢ Supporting Information

SDS−PAGE gels confirming the preparation of 40 kDa PEG conjugated trastuzumab and Alexa488 labeled PEG−trastuzumab and trastuzumab. Comparison between plasma concentrations of PEG−trastuzumab in non lymph cannulated and cannulated rats after intravenous and subcutaneous dosing. Observed vs individual or population fits of plasma concentrations or fractions of drug collected during one lymph sampling interval for both PEG−trastuzumab and trastuzumab. Slot blot images for anti PEG-protein IgM.

Permeability coefficients for PEG−trastuzumab or trastuzumab transfer from either apical-basal or basal-apical layers. This material is available free of charge via the Internet at http://pubs.acs.org.

AUTHOR INFORMATION

Corresponding Author

*E-mail: lisa.kaminskas@monash.edu. Tel: +61 3 9903 9522. Fax: +61 3 9903 9583.

Notes

The authors declare no competing financial interest.

REFERENCES

(1) Chames, P.; Van Regenmortel, M.; Weiss, E.; Baty, D. Therapeutic antibodies: successes, limitations and hopes for the future. *Br. J. Pharmacol.* **2009**, *157*, 220−33.

(2) Nelson, A. L.; Dhimolea, E.; Reichert, J. M. Development trends for human monoclonal antibody therapeutics. *Nat. Rev. Drug Discovery* **2010**, *9*, 767−74.

(3) Slamon, D.; Eiermann, W.; Robert, N.; Pienkowski, T.; Martin, M.; Press, M.; Mackey, J.; Glaspy, J.; Chan, A.; Pawlicki, M.; Pinter, T.; Valero, V.; Liu, M. C.; Sauter, G.; von Minckwitz, G.; Visco, F.; Bee, V.; Buyse, M.; Bendahmane, B.; Tabah-Fisch, I.; Lindsay, M. A.; Riva, A.; Crown, J. Breast Cancer International Research, G. Adjuvant trastuzumab in HER2-positive breast cancer. *N. Engl. J. Med.* **2011**, *365*, 1273−83.

(4) McKeage, K.; Perry, C. M. Trastuzumab: a review of its use in the treatment of metastatic breast cancer overexpressing HER2. *Drugs* **2002**, *62*, 209−43.

(5) Orman, J. S.; Perry, C. M. Trastuzumab: in HER2 and hormone receptor co-positive metastatic breast cancer. *Drugs* **2007**, *67*, 2781−9.

(6) Hazard, H.; Hansen, N. Sentinel Lymphadenectomy in Breast Cancer. In *Advances in Breast Cancer Management*, 2nd ed.; Gradishar, W., Wood, W., Eds.; Springer: New York, 2008; Vol. *141*, pp 11−36.

(7) Hack, T. F.; Cohen, L.; Katz, J.; Robson, L. S.; Goss, P. Physical and psychological morbidity after axillary lymph node dissection for breast cancer. *J. Clin. Oncol.* **1999**, *17*, 143−9.

(8) Giuliano, A. E.; Jones, R. C.; Brennan, M.; Statman, R. Sentinel lymphadenectomy in breast cancer. *J. Clin. Oncol.* **1997**, *15*, 2345−50.

(9) Chen, J.; Wang, L.; Yao, Q.; Ling, R.; Li, K.; Wang, H. Drug concentrations in axillary lymph nodes after lymphatic chemotherapy on patients with breast cancer. *Breast Cancer Res.* **2004**, *6*, R474−7.

(10) Dahlberg, A. M.; Kaminskas, L. M.; Smith, A.; Nicolazzo, J. A.; Porter, C. J. H.; Bulitta, J. B.; McIntosh, M. P. The lymphatic system plays a major role in the intravenous and subcutaneous pharmacokinetics of trastuzumab in rats. *Mol. Pharmaceutics* **2014**, *11*, 496−504.

(11) McLennan, D. N.; Porter, C. J. H.; Charman, S. A. Subcutaneous drug delivery and the role of the lymphatics. *Drug Discovery Today: Technol.* **2005**, *2*, 89−96.

(12) Kaminskas, L. M.; Kota, J.; McLeod, V. M.; Kelly, B. D.; Karellas, P.; Porter, C. J. H. PEGylation of polylysine dendrimers

improves absorption and lymphatic targeting following sc administration in rats. *J. Controlled Release* **2009**, *140*, 108−16.

(13) Kaminskas, L. M.; Ascher, D. B.; McLeod, V. M.; Herold, M. J.; Le, C. P.; Sloan, E. K.; Porter, C. J. H. PEGylation of interferon alpha2 improves lymphatic exposure after subcutaneous and intravenous administration and improves antitumour efficacy against lymphatic breast cancer metastases. *J. Controlled Release* **2013**, *168*, 200−8.

(14) Leveque, D. Subcutaneous administration of anticancer agents. *Anticancer Res.* **2014**, *34*, 1579−86.

(15) Shpilberg, O.; Jackisch, C. Subcutaneous administration of rituximab (MabThera) and trastuzumab (Herceptin) using hyaluronidase. *Br. J. Cancer* **2013**, *109*, 1556−61.

(16) Vugmeyster, Y.; Xu, X.; Theil, F. P.; Khawli, L. A.; Leach, M. W. Pharmacokinetics and toxicology of therapeutic proteins: Advances and challenges. *World J. Biol. Chem.* **2012**, *3*, 73−92.

(17) Kagan, L. Pharmacokinetic modeling of the subcutaneous absorption of therapeutic proteins. *Drug Metab. Dispos.* **2014**, *42* (11), 1890−905.

(18) Supersaxo, A.; Hein, W. R.; Steffen, H. Effect of molecular weight on the lymphatic absorption of water-soluble compounds following subcutaneous administration. *Pharm. Res.* **1990**, *7*, 167−9.

(19) Porter, C. J. H.; Charman, S. A. Lymphatic transport of proteins after subcutaneous administration. *J. Pharm. Sci.* **2000**, *89*, 297−310.

(20) Swartz, M. A.; Skobe, M. Lymphatic function, lymphangiogenesis, and cancer metastasis. *Microsc. Res. Tech.* **2001**, *55*, 92−9.

(21) Porter, C. J. H.; Edwards, G. A.; Charman, S. A. Lymphatic transport of proteins after s.c. injection: implications of animal model selection. *Adv. Drug Delivery Rev.* **2001**, *50*, 157−71.

(22) Swartz, M. A. The physiology of the lymphatic system. *Adv. Drug Delivery Rev.* **2001**, *50*, 3−20.

(23) McLennan, D. N.; Porter, C. J. H.; Edwards, G. A.; Brumm, M.; Martin, S. W.; Charman, S. A. Pharmacokinetic model to describe the lymphatic absorption of r-metHu-leptin after subcutaneous injection to sheep. *Pharm. Res.* **2003**, *20*, 1156−62.

(24) McLennan, D. N.; Porter, C. J. H.; Edwards, G. A.; Martin, S. W.; Heatherington, A. C.; Charman, S. A. Lymphatic absorption is the primary contributor to the systemic availability of Epoetin alfa following subcutaneous administration to sheep. *J. Pharmacol. Exp. Ther.* **2005**, *313*, 345−51.

(25) Charman, S. A.; McLennan, D. N.; Edwards, G. A.; Porter, C. J. H. Lymphatic absorption is a significant contributor to the subcutaneous bioavailability of insulin in a sheep model. *Pharm. Res.* **2001**, *18*, 1620−6.

(26) Charman, S. A.; Segrave, A. M.; Edwards, G. A.; Porter, C. J. H. Systemic availability and lymphatic transport of human growth hormone administered by subcutaneous injection. *J. Pharm. Sci.* **2000**, *89*, 168−77.

(27) Bumbaca, D.; Boswell, C. A.; Fielder, P. J.; Khawli, L. A. Physiochemical and biochemical factors influencing the pharmacokinetics of antibody therapeutics. *AAPS J.* **2012**, *14*, 554−8.

(28) Knop, K.; Hoogenboom, R.; Fischer, D.; Schubert, U. S. Poly(ethylene glycol) in drug delivery: pros and cons as well as potential alternatives. *Angew. Chem., Int. Ed.* **2010**, *49*, 6288−308.

(29) Baumann, A.; Tuerck, D.; Prabhu, S.; Dickmann, L.; Sims, J. Pharmacokinetics, metabolism and distribution of PEGs and PEGylated proteins: quo vadis? *Drug Discovery Today* **2014**, *19* (10), 1623−31.

(30) Deckert, P. M.; Jungbluth, A.; Montalto, N.; Clark, M. A.; Finn, R. D.; Williams, C., Jr.; Richards, E. C.; Panageas, K. S.; Old, L. J.; Welt, S. Pharmacokinetics and microdistribution of polyethylene glycol-modified humanized A33 antibody targeting colon cancer xenografts. *Int. J. Cancer* **2000**, *87*, 382−90.

(31) Kitamura, K.; Takahashi, T.; Yamaguchi, T.; Noguchi, A.; Noguchi, A.; Takashina, K.; Tsurumi, H.; Inagake, M.; Toyokuni, T.; Hakomori, S. Chemical engineering of the monoclonal antibody A7 by polyethylene glycol for targeting cancer chemotherapy. *Cancer Res.* **1991**, *51*, 4310−5.

(32) Banerjee, S. S.; Aher, N.; Patil, R.; Khandare, J. Poly(ethylene glycol)-Prodrug Conjugates: Concept, Design, and Applications. *J. Drug Delivery* **2012**, *2012*, 103973.

(33) Veronese, F. M. Peptide and protein PEGylation: a review of problems and solutions. *Biomaterials* **2001**, *22*, 405−17.

(34) Hayashi, Y.; Matsui, H.; Takagi, T. Membrane protein molecular weight determined by low-angle laser light-scattering photometry coupled with high-performance gel chromatography. *Methods Enzymol.* **1989**, *172*, 514−28.

(35) Ascher, D. B.; Wielens, J.; Nero, T. L.; Doughty, L.; Morton, C. J.; Parker, M. W. Potent hepatitis C inhibitors bind directly to NS5A and reduce its affinity for RNA. *Sci. Rep.* **2014**, *4*, 4765.

(36) Kaminskas, L. M.; Kelly, B. D.; McLeod, V. M.; Sberna, G.; Boyd, B. J.; Owen, D. J.; Porter, C. J. H. Capping methotrexate alpha-carboxyl groups enhances systemic exposure and retains the cytotoxicity of drug conjugated PEGylated polylysine dendrimers. *Mol. Pharmaceutics* **2011**, *8*, 338−49.

(37) Boyd, B. J.; Kaminskas, L. M.; Karellas, P.; Krippner, G.; Lessene, R.; Porter, C. J. H. Cationic poly-L-lysine dendrimers: pharmacokinetics, biodistribution, and evidence for metabolism and bioresorption after intravenous administration to rats. *Mol. Pharmaceutics* **2006**, *3*, 614−27.

(38) Girardet, R. E.; Benninghoff, D. L. Long term physiologic study of thoracic duct lymph and lymphocytes in rat and man. *Lymphology* **1977**, *10*, 36−44.

(39) Kaminskas, L. M.; McLeod, V. M.; Ascher, D. B.; Ryan, G. M.; Jones, S.; Haynes, J. M.; Trevaskis, N. L.; Chan, L. J.; Sloan, E. K.; Finnin, B. A.; Williamson, M.; Velkov, T.; Williams, E. D.; Kelly, B. D.; Owen, D. J.; Porter, C. J. H. Methotrexate-Conjugated PEGylated Dendrimers Show Differential Patterns of Deposition and Activity in Tumor-Burdened Lymph Nodes after Intravenous and Subcutaneous Administration in Rats. *Mol. Pharmaceutics* **2015**, *12* (2), 432−43.

(40) Ryan, G. M.; Kaminskas, L. M.; Bulitta, J. B.; McIntosh, M. P.; Owen, D. J.; Porter, C. J. H. PEGylated polylysine dendrimers increase lymphatic exposure to doxorubicin when compared to PEGylated liposomal and solution formulations of doxorubicin. *J. Controlled Release* **2013**, *172*, 128−36.

(41) Bulitta, J. B.; Bingolbali, A.; Shin, B. S.; Landersdorfer, C. B. Development of a new pre- and post-processing tool (SADAPT-TRAN) for nonlinear mixed-effects modeling in S-ADAPT. *AAPS J.* **2011**, *13*, 201−11.

(42) Bulitta, J. B.; Duffull, S. B.; Kinzig-Schippers, M.; Holzgrabe, U.; Stephan, U.; Drusano, G. L.; Sorgel, F. Systematic comparison of the population pharmacokinetics and pharmacodynamics of piperacillin in cystic fibrosis patients and healthy volunteers. *Antimicrob. Agents Chemother.* **2007**, *51*, 2497−507.

(43) Brendel, K.; Comets, E.; Laffont, C.; Laveille, C.; Mentre, F. Metrics for external model evaluation with an application to the population pharmacokinetics of gliclazide. *Pharm. Res.* **2006**, *23*, 2036−49.

(44) Bulitta, J. B.; Landersdorfer, C. B. Performance and robustness of the Monte Carlo importance sampling algorithm using parallelized S-ADAPT for basic and complex mechanistic models. *AAPS J.* **2011**, *13*, 9258−9259.

(45) Kaminskas, L. M.; McLeod, V. M.; Porter, C. J. H.; Boyd, B. J. Differences in colloidal structure of PEGylated nanomaterials dictate the likelihood of accelerated blood clearance. *J. Pharm. Sci.* **2011**, *100*, 5069−77.

(46) Owen, S. C.; Patel, N.; Logie, J.; Pan, G.; Persson, H.; Moffat, J.; Sidhu, S. S.; Shoichet, M. S. Targeting HER2+ breast cancer cells: lysosomal accumulation of anti-HER2 antibodies is influenced by antibody binding site and conjugation to polymeric nanoparticles. *J. Controlled Release* **2013**, *172*, 395−404.

(47) Hatakeyama, H.; Akita, H.; Harashima, H. A multifunctional envelope type nano device (MEND) for gene delivery to tumours based on the EPR effect: a strategy for overcoming the PEG dilemma. *Adv. Drug Delivery Rev.* **2011**, *63*, 152−60.

(48) Rath, T.; Kuo, T. T.; Baker, K.; Qiao, S. W.; Kobayashi, K.; Yoshida, M.; Roopenian, D.; Fiebiger, E.; Lencer, W. I.; Blumberg, R.

S. The immunologic functions of the neonatal Fc receptor for IgG. *J. Clin. Immunol.* **2013**, *33* (Suppl. 1), S9−17.

(49) Tzaban, S.; Massol, R. H.; Yen, E.; Hamman, W.; Frank, S. R.; Lapierre, L. A.; Hansen, S. H.; Goldenring, J. R.; Blumberg, R. S.; Lencer, W. I. The recycling and transcytotic pathways for IgG transport by FcRn are distinct and display an inherent polarity. *J. Cell Biol.* **2009**, *185*, 673−84.

(50) Roseng, L.; Tolleshaug, H.; Berg, T. Uptake, intracellular transport, and degradation of polyethylene glycol-modified asialofetuin in hepatocytes. *J. Biol. Chem.* **1992**, *267*, 22987−93.

(51) Roopenian, D. C.; Akilesh, S. FcRn: the neonatal Fc receptor comes of age. *Nat. Rev. Immunol.* **2007**, *7*, 715−25.

(52) Valabrega, G.; Montemurro, F.; Aglietta, M. Trastuzumab: mechanism of action, resistance and future perspectives in HER2-overexpressing breast cancer. *Ann. Oncol.* **2007**, *18*, 977−984.

(53) Gajria, D.; Chandarlapaty, S. HER2-amplified breast cancer: mechanisms of trastuzumab resistance and novel targeted therapies. *Expert Rev. Anticancer Ther.* **2011**, *11*, 263−75.

(54) Nahta, R. Molecular Mechanisms of Trastuzumab-Based Treatment in HER2-Overexpressing Breast Cancer. *ISRN Oncol.* **2012**, *2012*, 428062.

(55) Hudis, C. A. Trastuzumab—mechanism of action and use in clinical practice. *N. Engl. J. Med.* **2007**, *357*, 39−51.

(56) Longva, K. E.; Pedersen, N. M.; Haslekas, C.; Stang, E.; Madshus, I. H. Herceptin-induced inhibition of ErbB2 signaling involves reduced phosphorylation of Akt but not endocytic down-regulation of ErbB2. *Int. J. Cancer* **2005**, *116*, 359−67.

(57) Li, L.; Gardner, I.; Rose, R.; Jamei, M. Incorporating Target Shedding Into a Minimal PBPK-TMDD Model for Monoclonal Antibodies. *CPT: Pharmacometrics Syst. Pharmacol.* **2014**, *3*, e96.

(58) Kaminskas, L. M.; Porter, C. J. H. Targeting the lymphatics using dendritic polymers (dendrimers). *Adv. Drug Delivery Rev.* **2011**, *63*, 890−900.

(59) Zhan, X.; Tran, K. K.; Shen, H. Effect of the poly(ethylene glycol) (PEG) density on the access and uptake of particles by antigen-presenting cells (APCs) after subcutaneous administration. *Mol. Pharmaceutics* **2012**, *9*, 3442−51.

(60) Saifer, M. G.; Williams, L. D.; Sobczyk, M. A.; Michaels, S. J.; Sherman, M. R. Selectivity of binding of PEGs and PEG-like oligomers to anti-PEG antibodies induced by methoxyPEG-proteins. *Mol. Immunol.* **2014**, *57*, 236−46.

(61) Sherman, M. R.; Williams, L. D.; Sobczyk, M. A.; Michaels, S. J.; Saifer, M. G. Role of the methoxy group in immune responses to mPEG-protein conjugates. *Bioconjugate Chem.* **2012**, *23*, 485−99.

(62) Armstrong, J. K.; Hempel, G.; Koling, S.; Chan, L. S.; Fisher, T.; Meiselman, H. J.; Garratty, G. Antibody against poly(ethylene glycol) adversely affects PEG-asparaginase therapy in acute lymphoblastic leukemia patients. *Cancer* **2007**, *110*, 103−11.

(63) McLennan, D. N.; Porter, C. J. H.; Edwards, G. A.; Martin, S. W.; Charman, S. A. Molecular weight is a primary determinant for lymphatic absorption of proteins following subcutaneous administration to sheep. *AAPS PharmSci* **2002**, *4*, W4041.

(64) McLennan, D. N.; Porter, C. J. H.; Edwards, G. A.; Heatherington, A. C.; Martin, S. W.; Charman, S. A. The absorption of darbepoetin alfa occurs predominantly via the lymphatics following subcutaneous administration to sheep. *Pharm. Res.* **2006**, *23*, 2060−6.

(65) Kota, J.; Machavaram, K. K.; McLennan, D. N.; Edwards, G. A.; Porter, C. J. H.; Charman, S. A. Lymphatic absorption of subcutaneously administered proteins: influence of different injection sites on the absorption of darbepoetin alfa using a sheep model. *Drug Metab. Dispos.* **2007**, *35*, 2211−7.

(66) Oussoren, C.; Storm, G. Liposomes to target the lymphatics by subcutaneous administration. *Adv. Drug Delivery Rev.* **2001**, *50*, 143−56.